

RSC Advances



This is an *Accepted Manuscript*, which has been through the Royal Society of Chemistry peer review process and has been accepted for publication.

Accepted Manuscripts are published online shortly after acceptance, before technical editing, formatting and proof reading. Using this free service, authors can make their results available to the community, in citable form, before we publish the edited article. This *Accepted Manuscript* will be replaced by the edited, formatted and paginated article as soon as this is available.

You can find more information about *Accepted Manuscripts* in the [Information for Authors](#).

Please note that technical editing may introduce minor changes to the text and/or graphics, which may alter content. The journal's standard [Terms & Conditions](#) and the [Ethical guidelines](#) still apply. In no event shall the Royal Society of Chemistry be held responsible for any errors or omissions in this *Accepted Manuscript* or any consequences arising from the use of any information it contains.

ARTICLE

Redox-controlled fluorescence modulation (electrofluorochromism) in triphenylamine derivatives

Cite this: DOI: 10.1039/x0xx00000x

Received 00th January 2012,
Accepted 00th January 2012

DOI: 10.1039/x0xx00000x

www.rsc.org/

Cassandre Quinton, Valérie Alain-Rizzo,* Cécile Dumas-Verdes, Fabien Miomandre,* Gilles Clavier and Pierre Audebert

The study of the chemical and electrochemical fluorescence switching properties of a family of substituted triphenylamine derivatives is reported. First of all, the synthesis of a family of six compounds is described. They are characterized by electrochemistry, UV-vis and fluorescence spectroscopies and spectroelectrochemistry. Theoretical calculations were performed in order to corroborate the experimental results. While these compounds emit blue to green light under UV irradiation with a large quantum yield (37%) in the case of one molecule, the fluorescence intensity is quenched upon oxidation. The fluorescent behavior can be switched between strong fluorescent (neutral) state and non-fluorescent (oxidized) state with a high contrast (around 1500 for the fluorescence intensity for one of these molecules). Furthermore, the chromatic contrast of three of these molecules reaches 70% that can be important for further applications.

Introduction

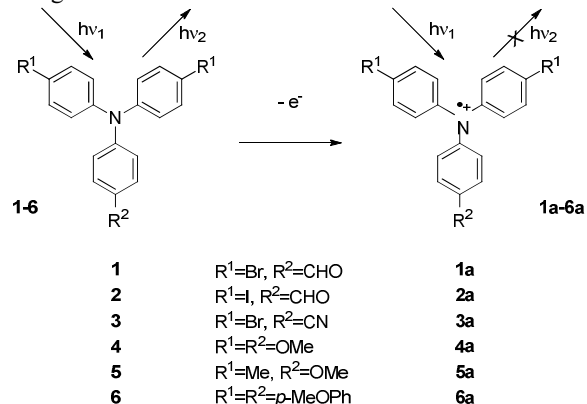
Reversible fluorescent switching by electrochemistry or electrofluorochromism¹ is an attractive field of research because of the several applications in biochemical issues,²⁻⁴ for the realization of electrofluorochromic windows⁵⁻⁸ or fluorescent sensors.⁹ Electrofluorochromic materials display a reversible optical change in the fluorescence resulting from electrochemical oxidation or reduction. Recently we showed interest in the study of tetrazine-triphenylamine bichromophores for their dual fluorescent switching application.^{10, 11} Such systems in which the fluorophore emission can be switched by changing the redox state of an active moiety connected to it has been already described in the literature.¹²⁻¹⁸ However, a straightforward fluorescence modulation can also be envisaged with an organic dye acting both as the light emitter and the redox switch.¹⁹⁻²⁴ Triphenylamines are well known derivatives used in electrochromism²⁵⁻³⁴ since they display most of the time

extremely stable cation-radicals^{35, 36} which can be formed at moderate oxidizing potential. Furthermore, depending on their substituents, the absorption and emission of triphenylamine can be tuned within all the visible region.³⁷⁻⁴⁰

Therefore triphenylamine derivatives constitute a family of very promising candidates for applications in electrofluorochromism. Indeed a study, which was made at the same time as ours, shows that conjugated polymers based on triphenylamine are successful materials for electrochemical fluorescence switching.⁴¹

We have prepared several triphenylamine derivatives bearing different groups on their para positions (Scheme 1) in order to investigate the influence of the nature of the substituent on their photophysical and electrochemical properties. In addition we performed theoretical quantum calculations to strengthen the analysis of the experimental results. We also investigated the photophysical behaviour (absorption and emission) of the triphenylaminium corresponding cation-radicals using either chemical or electrochemical oxidation depending on the

derivative. The aim of this work is not to develop highly sophisticated triphenylamine derivatives but at a more modest level to undertake a first step in the analysis of the structure-property relationships in various triphenylamine derivatives with as long-term goal the definition of guidelines for the future development of materials based on triphenylamine specifically designed for electrofluorochromism.



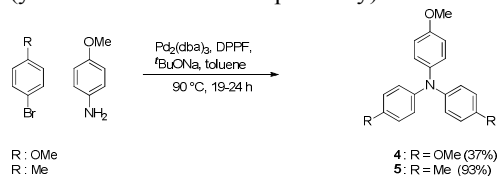
Scheme 1. Two redox states system of triphenylamine derivatives 1-6 with different fluorescence properties

Results and discussion

Synthesis

Design of substituted triphenylamines can be achieved employing two major strategies: either the synthesis of the triphenylamine core stems from substituted diphenylamines (Kaneko procedure) or primary phenylamines (Hartwig-Buchwald coupling), either functionalization (such as halogenation, Vilsmeier-Haack reaction or pallado-catalysed cross-coupling reaction) is performed on commercial triphenylamine derivatives. It should be reminded that though triphenylamines are well known to form stable cation-radicals, a free para position often lets them polymerize. Thus, to avoid polymerization during oxidation process, triphenylamine derivatives bearing substituents on para position were targeted. In order to study the influence of the electrodonating or electrowithdrawing behaviors of the substituents on photophysical properties, different groups were introduced: halides, cyano, methoxy, carbonyl, aryl.

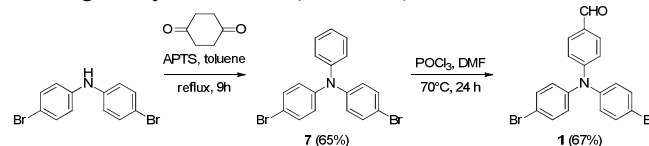
Thus targeted compounds **4** and **5** were obtained using a classical one-pot Hartwig-Buchwald procedure^{10, 42-45} (Scheme 2) on anisidine with excess of corresponding bromo derivatives (yields of 37 and 93% respectively).



Scheme 2. Synthesis of triphenylamine derivatives **4** and **5**

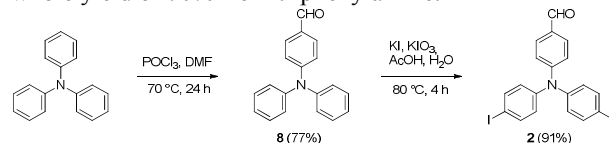
The original Kaneko condensation^{46, 47} of 1,4-cyclohexanedione on bis(4-bromophenylamine) led to the dibromotriphenylamine **7** (yield of 65%). This latter underwent a classical Vilsmeier-

Haack reaction⁴⁸⁻⁵⁰ affording the trisubstituted triphenylamine **1** with a global yield of 44% (Scheme 3).



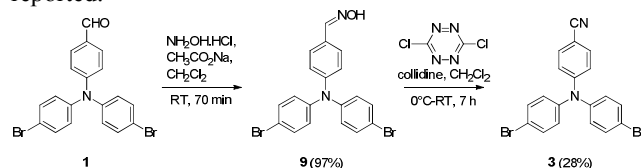
Scheme 3. Synthesis of triphenylamine derivative **1**

In order to enhance the global yield, another synthetic route has been employed to obtain the compound **2** starting from commercial triphenylamine as shown in Scheme 4. Triphenylamine was first monoformylated^{51, 52} in **8** with a Vilsmeier-Haack reaction (yield of 77%). The synthesis of **2** was achieved by the halogenation of **8** with iodine formed in situ from potassium iodide and potassium iodate leading to a whole yield of 70% from triphenylamine.⁵³



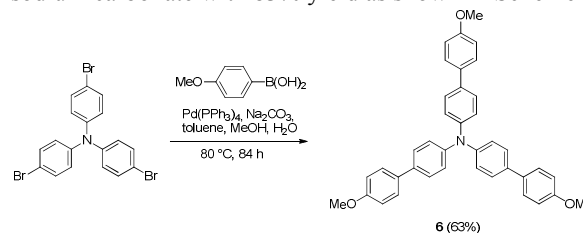
Scheme 4. Synthesis of triphenylamine derivative **2**

The synthetic procedure to the substituted triphenylamine **3** is outlined in Scheme 5. First hydroxylamine hydrochloride and sodium acetate action on aldehyde **1** led to the expected oxime **9** with a very good yield (97%).⁵⁴ Then nitrile **3** was synthesized through an original Beckmann transposition of intermediary oxime **9** formed by nucleophilic aromatic monosubstitution of 3,6-dichloro-*s*-tetrazine with oxime **9**. Conversion of aldoxime to nitrile is well known,⁵⁵⁻⁵⁹ however it must be noted that the utilization of 3,6-dichloro-*s*-tetrazine as an activator in a Beckmann transposition has never been reported.



Scheme 5. Synthesis of triphenylamine derivative **3** through a Beckmann type rearrangement

Finally, the last compound **6** was synthesized by functionalization of commercially available *N,N,N*-tri-(4-bromophenyl)amine through a Suzuki-Miyaura cross-coupling⁶⁰ with methoxyphenylboronic acid using Pd(PPh₃)₄ as the catalyst in a mixture of toluene, methanol and aqueous sodium carbonate with 83% yield as shown in Scheme 6.



Scheme 6. Synthesis of triphenylamine derivative **6**

Hence, the syntheses of six triphenylamine derivatives have been successfully realized in few steps and relatively good global yields.

Electrochemical investigations

Cyclic voltammetry (CV) was used to investigate the electrochemical behavior of the different triphenylamine compounds. As expected, CV shows one-electron fully reversible oxidation of triphenylamine into its cation-radical (see Figure 1 for **2** and **4** and supporting information for **1**, **3**, **5** and **6**).

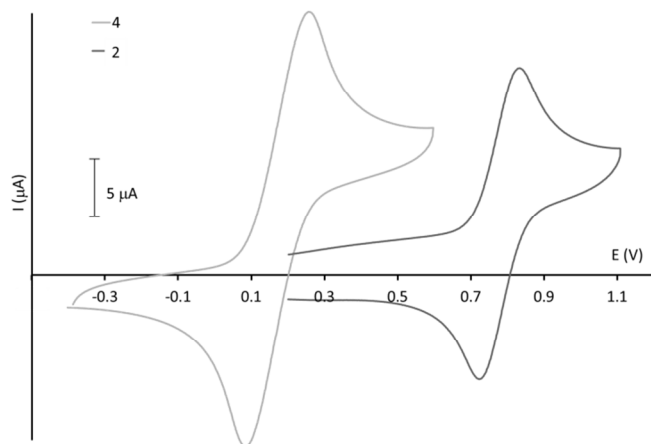


Figure 1. Cyclic voltammetry of compounds **2** and **4** in dichloromethane (10^{-5} mol.L $^{-1}$) + 0.1M TBAPF $_6$ on glassy carbon. Potentials referenced to ferrocene. Scan rate: 100 mV.s $^{-1}$

The effects of the substituent on the triphenylamine core on the oxidation potential were examined and the data are gathered in Table 1. The oxidation potential values are much lower in the case of electrodonating substituents (**4**, **5** and **6**) than in the case of electrowithdrawing substituent (**1**, **2** and **3**) as expected. In fact, electrodonating groups like methyl, methoxy and methoxyphenyl groups lead to an easier oxidation than electrowithdrawing groups like aldehyde, nitrile or halide groups. Therefore electrodonating substituents lead to a cathodic shift in triphenylamine oxidation potential compared to the one of the triphenylamine estimated at 0.47 V vs. ferrocene.⁶¹⁻⁶³ The extension of the conjugated link increases a little the oxidation potential value as seen for molecules **6** (vs. **4**) because the methoxy group is farther. Conversely, the change of a bromine atom for an iodine atom does not modify the oxidation behavior (molecules **1** and **2**).

Table 1. Electrochemical data for compounds **1-6**: standard potential E $^{\circ}$, anodic peak potential Epa, cathodic peak potential Epc and $\Delta E_p = E_{pa} - E_{pc}$. Potentials are referenced to ferrocene. All measurements in dichloromethane + TBAPF $_6$ on glassy carbon.

Compounds	1	2	3	4	5	6
E $^{\circ}$ (V)	0.79	0.78	0.85	0.17	0.22	0.25

Epa (V)	0.84	0.83	0.93	0.26	0.34	0.30
Epc (V)	0.75	0.72	0.77	0.08	0.09	0.20
ΔE_p (V)	0.09	0.11	0.16	0.18	0.25	0.10

As a conclusion and as expected, the compounds **4**, **5** and **6** can be easily oxidized with a mild chemical oxidant whereas the compounds **1**, **2** and **3** require electrochemical oxidation, as no colorless one-electron chemical oxidant is available in this potential range. Thus, in the case of **4**, **5** and **6**, the color can be changed at lower potential (using less energy) than for reported electrochromic triphenylamine based polymers.²⁵

Photophysical studies

The UV-vis absorption and the fluorescence spectra of **4** in acetonitrile are shown in Figure 2 and the photophysical data of the triphenylamine derivatives are summarized in Table 2.

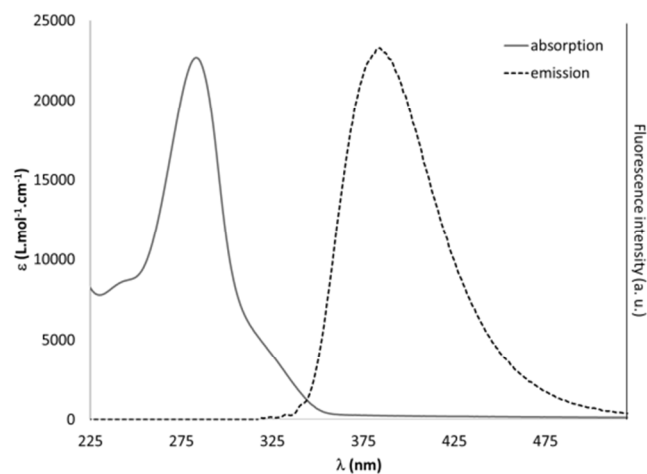


Figure 2. Absorption (solid line) and fluorescence emission (dash line, excitation wavelength: $\lambda_{exc} = 309$ nm) spectra of **4**

These compounds display one intense band in the UV region in agreement with a $\pi-\pi^*$ transition localized on the phenyl rings (see theoretical calculations). It should be noted that in the case of **6**, the molar absorption coefficient is nearly twice the one of the other triphenylamine derivatives. Indeed **6** contains six phenyl rings whereas the others only three. Depending on the substituent, the maximum of the absorption band is found between 283 and 357 nm. Under UV irradiation, all these triphenylamine derivatives show fluorescence emission and the maximum of this emission band varies between 382 and 532 nm depending on the substituent. The fluorescence band shape is a good mirror image of the absorption one. Quantum yields are listed in Table 2 for compounds **1-6** by comparison against quinine sulfate in H $_2$ SO $_4$ ($\Phi = 0.546$).⁶⁴ The quantum yields are around 0.05 except for **6**, for which the quantum yield is much higher (0.37). The values of the lifetime is found in the same range for all compounds, between 0.9 and 3.6 ns depending of the substituent, as already reported.⁶⁵

Exchanging the bromine into an iodine atom does not change the absorption and emission wavelengths (**1** vs. **2**). However,

the quantum yield and the lifetime are decreased because of a stronger heavy atom effect (favouring spin-orbit coupling to the non-emissive triplet state) with the iodine atom. Furthermore, if we compare compounds **1** and **3**, we can observe a blue-shift of the absorption and emission bands from **1** to **3** because of a less important intramolecular charge transfer from the nitrogen of the triphenylamine to the electrowithdrawing groups (see theoretical calculations).

Contrariwise, increasing the strength of the electrodonating groups from **5** to **4** leads to a slight blue-shift of the absorption band in agreement with a donor-donor built compound. In addition, increasing the conjugation length of the link by one phenyl ring in each branch from **4** to **6** leads to a red-shift of the bands.

Table 2. Photophysical properties for the triphenylamine derivatives **1-6** in acetonitrile: absorption wavelength [λ_{abs} , nm], molar absorption coefficient [ϵ , L.mol⁻¹.cm⁻¹], emission wavelength [λ_{em} , nm], fluorescence quantum yield [Φ], lifetime [τ , ns].

Compounds	λ_{abs}	ϵ	λ_{em}	Φ	τ
1	353	22500	531	0.06	2.7
2	355	24100	532	0.04	0.9
3	311	22700	447	0.09	1.5
4	283	22500	384	0.06	3.6
5	301	25000	382	0.03	1.8
6	357	54300	418	0.37	1.7

So all these triphenylamine derivatives are fluorescent, although sometimes with moderate yields, and are good candidates for fluorescent switching. Depending on the substituents, absorption and emission wavelengths can be tuned.

Chemical fluorescence switching and electrochromism

As previously mentioned, these triphenylamine derivatives are fluorescent in the blue to the green region in their neutral state. The generation of triphenylaminium cation can be achieved either by electrochemical or chemical oxidation. The first set of experiments involved a one-electron chemical oxidation: Cu(ClO₄)₂ was used as a mild and clean oxidant and has been recently reported to effectively generate arylaminium cation-radicals.^{10, 11, 66-68} Another advantage of using Cu(ClO₄)₂ is that it gives no absorption or emission in the UV-visible domain at low concentrations and its reduction potential in acetonitrile is 0.7 V vs. Fc/Fc⁺, which matches well with the oxidation potentials of **4**, **5** and **6**. The cation-radicals of the triphenylamine derivatives are thus generated using Cu(ClO₄)₂ in acetonitrile, this being the most suitable solvent to dissolve

both the oxidant and the triphenylamine derivatives, and are characterized by absorption and emission spectroscopies.

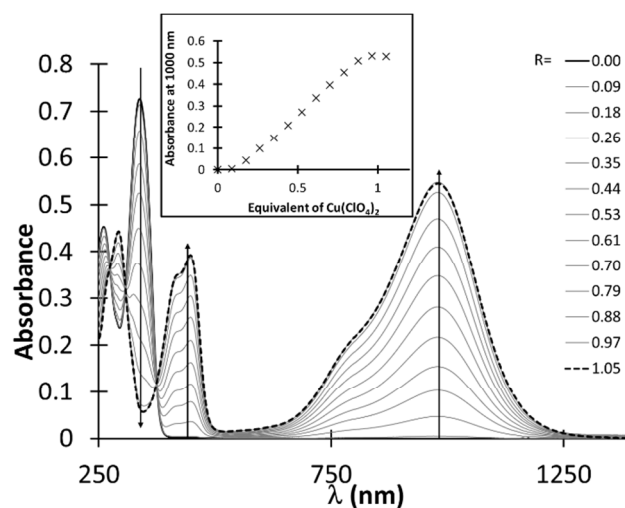


Figure 3. Absorption spectra recorded upon oxidation of **6** by Cu(ClO₄)₂ in CH₃CN as a function of R=[Cu^{II}]/[**6**], [**6**]=4.8 10⁻⁶ mol.L⁻¹. Inset: Correlation of the absorbance at 1000 nm with the amount of Cu(ClO₄)₂.

Upon titration with Cu(ClO₄)₂, the absorption band in the UV region decreases whereas two bands gradually appear at 360 and 759 nm for **4**, 360 and 706 nm for **5** and 450 nm and 980 nm for **6** (Figure 3; Supporting Information for **4** and **5**). The new absorption bands are attributed to the formation of the cation-radical. One can also observe the appearance of two isosbestic points at 245 and 309 nm for **4**, 263 and 323 nm for **5** and 307 and 374 nm for **6** in agreement with the existence of an equilibrium between the triphenylamine derivative and its cation-radical. The correlation of the absorbance for the lower energy band with the amount of Cu(ClO₄)₂ reveals that oxidation is complete when 1.4 equivalents of Cu(ClO₄)₂ is added for **4**, 1.5 for **5** and 1.0 for **6** (inset in Figure 3; Supporting Information for **4** and **5**). Conversely, even an excess of Cu(ClO₄)₂ does not oxidize **1**, **2** or **3** whose standard potentials are too high, in accordance with the electrochemical studies.

One important characteristic of electrochromic materials is the chromatic contrast ($\Delta T\%$), which can be defined as the transmittance difference between the redox states. These values are gathered in Table 3. If chromatic contrast is rather low in the case of **3** (17 and 16% at 719 and 364 nm respectively), the donating triphenylamine **4**, **5** and **6** display higher values (around 70% at low energy and around 50% at high energy) than conjugated systems derived from thienyl-derivatized poly(triphenylamine)s³⁰ and triphenylamine-based multielectrochromic material.³¹

Table 3. Chromatic contrast ($\Delta T\%$) for the triphenylamine derivatives **1-6** in acetonitrile:

Compounds	λ (nm)	$\Delta T\%$
3	719	17

	364	16
4	759	73
	360	44
5	706	69
	369	49
6	980	71
	447	59

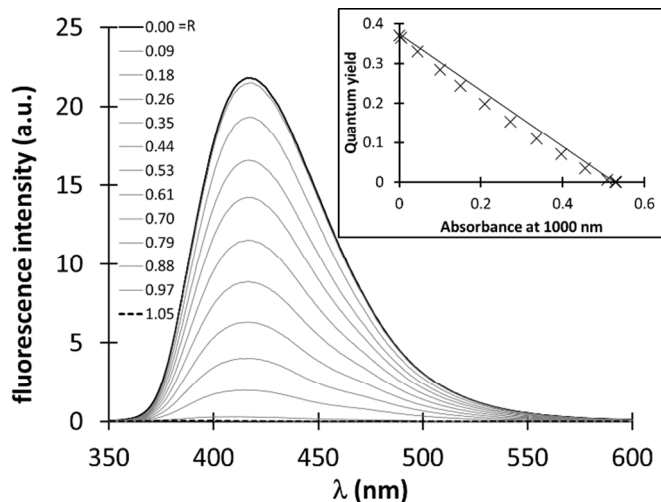


Figure 4. Fluorescence emission spectra recorded upon oxidation of **6** by $\text{Cu}(\text{ClO}_4)_2$ in CH_3CN as a function of $R = [\text{Cu}^{\text{II}}]/[\mathbf{6}]$, $[\mathbf{6}] = 4.8 \times 10^{-6} \text{ mol.L}^{-1}$, $\lambda_{\text{exc}} = 307 \text{ nm}$. Inset: Correlation of the quantum yield with the absorbance at 1000 nm.

Figure 4 displays the fluorescence emission evolution of **6** upon oxidation. The excitation wavelength was chosen at 307 nm, one of the isosbestic points. Upon oxidation by $\text{Cu}(\text{ClO}_4)_2$, the fluorescence emission of **6** was gradually decreased and completely quenched for 1.05 equivalents of oxidant, which is relevant to the formation of the non-fluorescent cation-radical. Thus, the fluorescence intensity at the maximum is divided by 1425 for **6**. The inset in Figure 4 represents the correlation of the fluorescence quantum yield of **6** with the absorbance at 1000 nm, which is characteristic of the cation-radical. One can observe an almost linear fluorescence quenching upon increasing the cation-radical concentration. The deviation from linearity can be attributed to a possible quenching through energy transfer of the triphenylamine derivative fluorescence by its own cation-radical. One can in addition state that it is a static quenching because of the results in time-resolved emission experiments. The value of the lifetime is always the same whatever the oxidation level ratio, only the intensity decreases.

For molecules **4** and **5**, one can observe the same behavior even if the fluorescence emission is not totally quenched in these two cases (see supporting information).

In order to test the reversibility of the systems and to check the fluorescence switching in the case of **1**, **2** and **3**, spectroelectrochemical studies were performed

Absorption spectroelectrochemistry of **3** was performed in a tailored thin layer spectroelectrochemical cell and the results

shown in figure 5. Upon oxidation (Figure 5a), two main bands are growing, located respectively at 370 and 710 nm, while the main band of the neutral species at 310 nm (see supporting information) gradually disappears. The long wavelength absorption band which appears upon oxidation is characteristic of the cation-radical form with a charge transfer character but less marked than for other triphenylamine derivatives⁶⁹ since no absorption in the NIR region is observed. The presence of two isosbestic points at 270 and 330 nm evidences the conversion of **3** into its cation-radical form. Upon reduction (Figure 5b), the variation in opposite directions can be observed (except for the high energy band at 230 nm that still grows), showing that the electrochemical reaction is actually reversible.

Fluorescence spectroelectrochemistry (electrofluorochromism) for the same compound was performed in the same cell with an excitation wavelength close to the isosbestic point at 330 nm. A broad emission band centered around 450 nm is observed under open circuit potential (supporting information). When recording the emitted light at this wavelength as a function of time when a linear potential scan is applied to the electrode, the fluorescence intensity shows a dramatic drop, followed by partial recovery when the potential is swept back to the initial value (Figure 6). This behavior is expected when compared to other triphenylamine compounds,⁶⁹ which were shown to fluoresce at the neutral state and not in their first oxidation state. However it can be noticed that the recorded fluorescence gradually decreases at the beginning of the scan, whereas no change in the redox state is induced by the potential in that range. A photobleaching when exciting in the UV is likely to explain this instability. This is also the reason why the recovered fluorescence intensity at the end of the backward scan is significantly lower than the initial value, although there is also a contribution in this difference coming from the electrochemical reaction (the final current is also lower than the initial one, showing remaining oxidized form at the end of the scan).

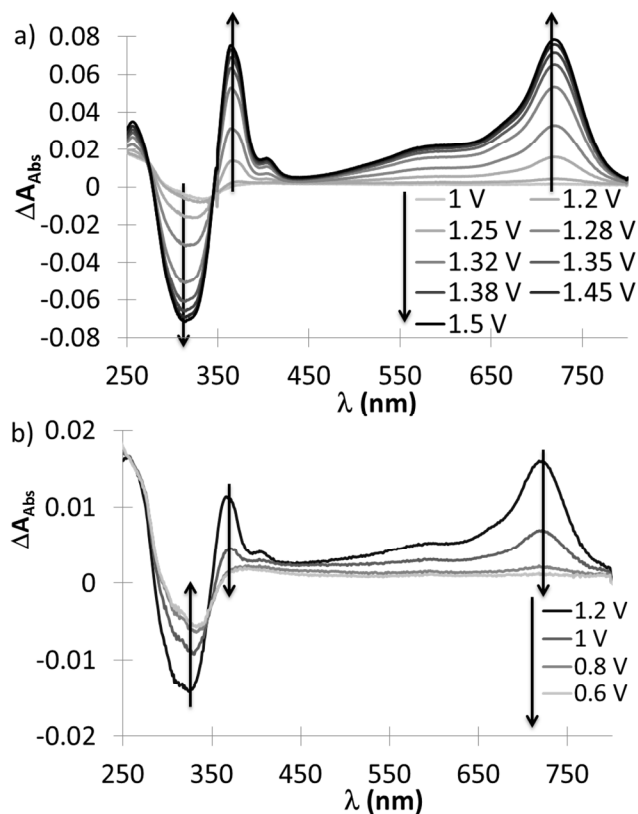


Figure 5. UV-Vis spectroelectrochemistry of **3** in acetonitrile (7.10^{-4} M) + TBAPF₆ at various potentials: a) from 1.2 to 1.5 V, b) from 1.2 to 0.6 V. The open circuit spectrum is used as the background and subtracted from all the other subsequent spectra.

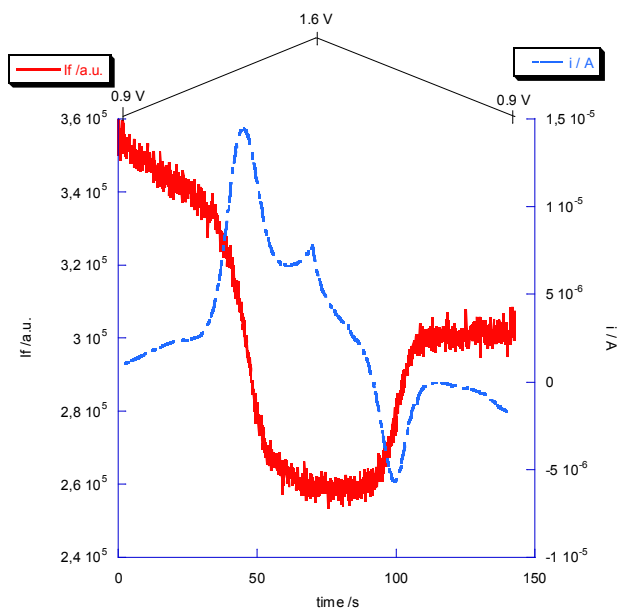


Figure 6. Variation of fluorescence intensity (red curve) of **3** with time upon application of a linear potential scan from 0.9 to 1.6 V (10 mV/s). The corresponding current vs. time is shown (dashed blue curve) extracted from the CV (inset).

For comparison sake, fluorescence spectroelectrochemistry of **1** was also recorded. The variation of fluorescence intensity at 530 nm when exciting at 350 nm upon a linear potential scan from 1.0 to 1.6 V is shown in Figure 7. A similar trend is observed but this time the fluorescence intensity remains constant when there is no change in the redox state. Unfortunately, the electrogenerated cation-radical of **1** is not stable enough at longer times to record absorption spectroelectrochemistry. A progressive consumption of the reactant is observed leading to a strong decreasing signal both in fluorescence and electrochemistry. This is confirmed by UV-vis spectroelectrochemistry that shows progressive disappearance of the bands of **1** upon electrochemical oxidation without any isosbestic points (see supporting information).

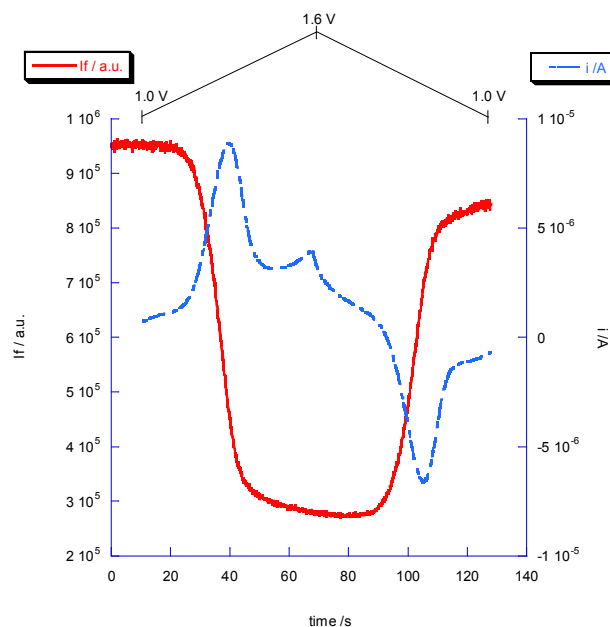


Figure 7. Variation of fluorescence intensity (red curve) of **1** with time upon application of a linear potential scan from 1.0 to 1.6 V (10 mV/s). The corresponding current vs. time is shown (dashed blue curve) extracted from the CV (inset).

Finally these triphenylamine derivatives unambiguously lead to a reversible switching of fluorescence and thus behave as on-off two-state systems.

Theoretical calculations

Quantum chemical calculations were carried out on triphenylamine derivatives **1-6**. Geometry optimizations were first performed at the B3LYP level of theory and with the 3-21g basis set. Time-dependent density functional theory (TD-DFT) calculations⁷⁰ at the PBE0 level of theory with the 6-31+g(d) basis set were subsequently performed.

For all these derivatives, the highest occupied molecular orbital (HOMO) is always a π -orbital delocalized on the entire molecule. The lowest unoccupied orbital (LUMO) is a π^* -orbital delocalized on one, two or three branches and onto the

terminal group in the case of electrowithdrawing CN and CHO groups, only with a weak coefficient on the central nitrogen. All compounds show one absorption band close to the UV-region. This absorption band is due to two types of transition for the triphenylamines **1**, **2** and **3** substituted by CHO or CN attracting groups. In the case of **1** and **3**, one transition ($\lambda_{th}=357$ and 333 nm respectively) is from the HOMO to the LUMO localized on the electron-withdrawing substituted branch and the other ($\lambda_{th}=310$ and 309 nm respectively) is from the HOMO to the π^* -orbital (L+2) localized on the two other branches (Figure 8). Absorption spectra constructed from these theoretical data gave calculated absorption maxima at 357 and 328 nm for **1** and **3** respectively (Table 3). The charge transfer HOMO-LUMO transition is estimated at 357 nm for **1** and 333 nm for **3** in agreement with the observed hypsochromic shift from **1** to **3**. In the case of **2**, the absorption band is due to the HOMO-LUMO and HOMO-L+4 transitions. In case of **5**, two transitions are also responsible for the absorption band: one from the HOMO to π^* -orbital (L+1) localized on two tolyl groups and the other from the HOMO to the π^* -orbital (L+2) localized on the methoxyphenyl group. Because of C3 symmetry, **4** and **6** have degenerated orbitals which increase the number of orbitals involved in the transitions. In the case of **4**, two transitions (with three contributions for each transition, see the supporting information) can be noted from the HOMO to the π^* -orbitals L+1, L+2, L+3 and L+4. In the case of **6**, there are transitions from HOMO, H-1 and H-2 π -orbitals to both LUMO and L+1 π^* -orbitals. Representation of the molecular orbitals involved in the electronic transitions of compounds **1-2,4-6** are available in the supporting information.

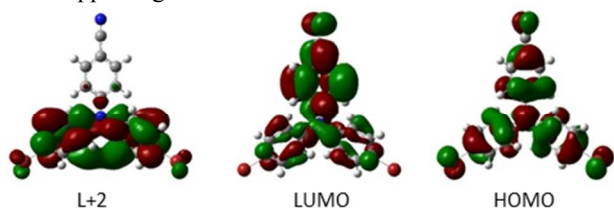


Figure 8. Representation of the main molecular orbitals involved in the electronic transitions of **3**.

We can notice that wavelength calculations fit well with experimental ones in the case of **1**, **2** and **3** but are overestimated in the case of electrodonating substituted triphenylamines **4**, **5** and **6** (Table 4). Furthermore calculations confirm that the molar absorption coefficient of **6** is nearly twice that of the other triphenylamine derivatives, as mentioned above.

Table 4. Experimental and calculated absorption wavelength (λ_1 , nm), molar absorption coefficient (ϵ_1 , $L \cdot mol^{-1} \cdot cm^{-1}$) for **1-6** (λ_1 , ϵ_1) and their respective cation-radicals (λ_2 and λ_3).

	λ_{1exp}	λ_{1cal}	ϵ_{1exp}	ϵ_{1cal}	λ_{2exp}	λ_{2cal}	λ_{3exp}	λ_{3cal}
1	353	357	22500	36000	nd ^a	365	715	692
2	355	349	24100	37500	nd ^a	344	777	798
3	311	328	22700	42200	364 ^b	361	719 ^b	697

4	283	363	22500	35300	360	352	759	658
5	301	362	25000	32100	360	347	706	630
6	357	433	54300	70500	450	420	980	1130

^a non-determined, ^b estimated by spectroelectrochemistry

Quantum chemical calculations were also done on the cation-radicals **1-6a** of triphenylamine derivatives **1-6**. All oxidized triphenylamine derivatives show two absorption bands: one is located in the near IR-region and the other one is around 400 nm (see Figure 3 for **6** and supporting information for **4** and **5**). The weak energy band is due to transitions whose contributions are from lower levels to the single occupied molecular orbital (SOMO) whereas the visible transition is due to transitions from SOMO to higher orbitals (see Figure 9 for **5** and supporting information for the other compounds). In the case of **1** and **3**, other orbitals are also involved in the second band. In the case of **1** and **3**, other orbitals are also involved in the second band with transitions from S-10 to SOMO and from S-2 to S+1 contributing.

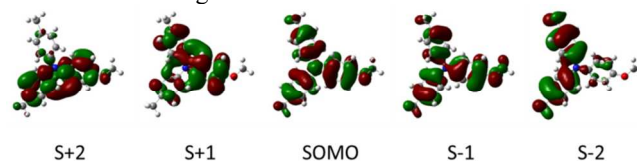


Figure 9. Representation of the main molecular orbitals involved in the electronic transitions of the cation-radical of **5**.

Conclusions

Several triphenylamine derivatives have been synthesized and their photophysical and electrochemical properties have been investigated. The generation of triphenylaminium cations could be achieved by either chemical oxidation or electrochemistry and their photophysical properties have been investigated too. As already known, triphenylamine derivatives could exhibit moderate to high fluorescence quantum yields in their neutral state whereas their cation-radicals are not fluorescent. In conclusion, it has been possible to produce a reversible fluorescence switch by using triphenylamine derivatives. This fluorescent switching can be achieved for both electroattracting and electrowithdrawing substituted triphenylamine, but the use of donor group is recommended for the fabrication of electrofluorochromic materials since the radical-anion is thus more stable. Furthermore, a highly fluorescent triphenylamine derivative should be chosen in order to get an important fluorescent contrast. Finally, redox potential and fluorescence wavelength and intensity can be tuned according to the nature of the substituent on the triphenylamine core thanks to the considerable work which has already been done on triphenylamine derivatives. A multi-color electrofluorochromism could therefore be achieved using carefully chosen types of triphenylamine derivatives. At neutral state the solution should emit the color of the two fluorophores mixed together. Above first oxidation potential, only one triphenylamine compound could be fluorescent. If all

triphenylamine derivatives are oxidized, this system should be off. This could open the way toward original multi-state electrofluorochromic devices.

Experimental Section

Spectroscopic measurements

UV-visible absorption spectra were recorded on a Cary 5000 spectrophotometer in 1 cm optical length quartz cuvettes. Corrected emission spectra were obtained on a Jobin–Yvon Horiba Spex FluoroMax-3 spectrofluorometer. Acetonitrile (SDS, spectrometric grade) was employed as the solvent for absorption and fluorescence measurements. The fluorescence quantum yields were determined by using quinine sulfate in H₂SO₄ (0.5 N) as a standard ($\Phi_f=0.546$). The estimated experimental error is less than 10%. For the emission measurements, a right-angle configuration was used. Fluorescence decay curves in solution were obtained using a time-correlated single-photon counting method using a titanium-sapphire laser pumped by an argon ion laser (Tsunami, by Spectra-Physics, 82 MHz, 1 ps pulse width, repetition rate lowered to 4 MHz with a pulse-peaker, a doubling crystal was used to reach 495 nm excitation). The Levenberg–Marquardt algorithm was used for the non-linear least-squares fit. Copper (II) perchlorate hexahydrate was commercially available from Aldrich.

Electrochemistry

Solvents (SDS, HPLC grade) and electrolyte salts (tetrabutylammonium hexafluorophosphate from Fluka, puriss.) were used without further purification. Cyclic voltammetry was performed in a three-electrode cell with a potentiostat (VersaSTAT4, Princeton Applied Research) driven by a PC. Glassy carbon electrode (1 mm diameter) was used as the working electrode, whereas platinum wire and Ag⁺ (0.01 M in acetonitrile)/Ag were used, respectively, as the counter and reference electrodes. All the investigated solutions were deaerated by argon-bubbling for at least 2 min before performing the electrochemical measurements. The reference electrode was checked versus ferrocene as recommended by IUPAC.

Quantum Chemical Calculations

Calculations were performed with the Gaussian 03 at the MESO calculation centre of the ENS Cachan (Nec TX7 with 32 processors of type Itanium 2). Molecules were drawn with the Gaussview 03 software using included templates and their geometry optimized at the B3LYP/3-21+g(d) level of theory (LANL2DZ for the iodine atoms). Infrared spectra were calculated on the final geometry to ascertain that a minimum was obtained (no negative frequencies). Time-dependant density functional theory (TD-DFT) calculations at the PBE0 level of theory with the 6-31+g(d) basis set (LANL2DZ for the iodine atoms) were subsequently performed. Reconstructed

absorption spectra have been obtained by convolution of Gaussian functions for each calculated transition with a full width at half maximum (FWHM) of 3000 cm⁻¹ and a surface equals to the oscillator strength as implemented in GaussSum. The ϵ_{calc} was thus obtained at the maximum of the band.

Electrofluorochromism

A thin layer electrochemical cell⁷¹ (sodium chloride windows, Pt minigrad working electrode, Ag pseudo-reference, Pt counter-electrode, optical path ca. 200 μm) was filled with the solution of the compound of interest. For fluorescence spectroelectrochemistry, excitation and emission were focused on the working electrode through optical fibers connected to a Jobin–Yvon Fluorolog 3 spectrophotometer. The fluorescence near the maximum emission wavelength was recorded vs. time simultaneously to the current corresponding to low scan rate cyclic voltammetry (10 mV/s). The electrochemical cell was connected to a CHI Instruments (CHI 600) potentiostat driven by a PC. For UV-vis spectroelectrochemistry, the thin layer cell was directly inserted in the spectrophotometer (Cary 5000, Varian). The spectrum for open circuit potential is recorded and used as the background for all other subsequent spectra.

Synthesis

Reagents were commercially available from Aldrich and used without further purification. Column chromatography was performed with SDS 0.040-0.063 mm silica gel. All compounds were characterized by the usual analytical methods: ¹H, ¹³C NMR spectra were recorded with a JEOL ECS (400 MHz) spectrometer. All chemical shifts are referenced to the solvent peak (J values are given in Hz). Melting points were measured with a Kofler melting-point apparatus. IR spectra were recorded with a Nicolet Avatar 330 FT-IR spectrometer. This work has benefited from the facilities and expertise of the Small Molecule Mass Spectrometry platform of IMAGIF (Centre de Recherche de Gif - www.imagif.cnrs.fr).

4-[N,N-di-(4'-bromophenyl)amino]benzaldehyde 1: To a solution of phosphorus oxychloride (1.5 mL, 16 mmol, 4.4 eq) in dimethylformamide (7.0 mL, 91 mmol, 24 eq) at 0°C under argon was added bis(4-bromophenyl)phenylamine (1.50 g, 3.72 mmol, 1.0 eq). The mixture was stirred at 70°C for 60 h. The mixture was then poured into the ice and neutralised with saturated sodium carbonate solution (20 mL). The aqueous layer was extracted with CH₂Cl₂ (3*20 mL). The organic layer was dried over anhydrous sodium sulfate, filtered and concentrated under reduced pressure. The crude product was purified by a silica gel flash chromatography [DCM/PE (5/5)] to give **1** (1.17 g, 67%) as yellow solid. ¹H NMR (400 MHz, CDCl₃) δ (ppm): 9.84 (s, 1H), 7.71 (d, J=8.7 Hz, 2H), 7.44 (d, J=9.2 Hz, 4H), 7.04 (d, J=8.7 Hz, 2H), 7.02 (d, J=8.7 Hz, 4H); ¹³C NMR (100 MHz, CDCl₃) δ (ppm): 190.5, 152.4, 145.1, 133.0, 131.5, 130.2, 127.5, 120.5, 118.2; IR (σ in cm⁻¹): 1486, 1073; m.p.: 154°C (lit.⁵⁰ 155-156); UV-vis (CH₃CN): λ_{max} (ϵ) = 353 (22500 L.cm⁻¹.mol⁻¹); $\Phi_f=0.06$ in CH₃CN; $\tau=2.67$ ns; E° (C, CH₂Cl₂) vs. ferrocene: 0.79 V.

4-[*N,N*-di-(4'-iodophenyl)amino]benzaldehyde 2: To a solution of 4-(*N,N*-diphenylamino)benzaldehyde **8** (5.01 g, 18.3 mmol, 1.0 eq) in water (20 mL) were added potassium iodide (3.97 g, 23.9 mmol, 1.3 eq) and acetic acid (80 mL). The mixture was warmed at 80°C and then potassium iodate (3.93 g, 18.4 mmol, 1.0 eq) was added. The mixture was stirred at 80°C for 4 h. The reaction mixture was cooled to room temperature and the solid product was filtrated and washed with ethanol. It was recrystallized in ethanol/dichloromethane to give **2** as a white solid (8.74 g, 91 %). ¹H NMR (400 MHz, CDCl₃) δ (ppm): 9.84 (s, 1H), 7.71 (d, J=8.7 Hz, 2H), 7.63 (d, J=8.7 Hz, 4H), 7.05 (d, J=8.7 Hz, 2H), 6.89 (d, J=8.7 Hz, 4H); ¹³C NMR (100 MHz, CDCl₃) δ (ppm): 190.6, 152.4, 145.8, 139.0, 131.5, 130.4, 127.8, 120.9, 88.9; IR (σ in cm⁻¹): 1693, 1600, 1574, 1483, 1316, 1270, 1216, 1163, 1064, 817; m.p.: 144°C (lit.⁷² 144); UV-vis (CH₃CN): λ_{max}(ε) = 313 (18400 L.cm⁻¹.mol⁻¹), 355 (24100 L.cm⁻¹.mol⁻¹); Φ_F=0.04 in CH₃CN; τ=1.16 ns; E° (C, CH₂Cl₂) vs. ferrocene: 0.78 V.

4-[*N,N*-bis-(4'-bromophenyl)amino]benzoxime 3: To a solution of 4-[*N,N*-di-(4-bromophenyl)amino]benzaldehyde oxime **9** (200 mg, 0.45 mmol, 1.0 eq) in anhydrous CH₂Cl₂ (0.05 M) were added 3,6-dichlorotetrazine (68 mg, 0.45 mmol, 1.0 eq) and 2,4,6-collidine (60 μL, 0.45 mmol, 1.0 eq). The mixture was stirred at room temperature for 3.5 hours then concentrated under reduced pressure. The crude product was purified by a silica gel flash chromatography [DCM/PE (5/5)] to give **9** (53 mg, 28 %) as white solid. ¹H NMR (400 MHz, CDCl₃) δ (ppm): 7.47-7.39 (m, 6H); 6.94-7.01 (m, 6H); ¹³C NMR (100 MHz, CDCl₃) δ (ppm): 150.8, 144.9, 133.5, 133.1, 127.4, 120.8, 119.3, 118.3, 104.2; IR (σ in cm⁻¹): 3205-2922, 2214, 1604, 1579, 1503, 1482, 1313, 1287, 1268, 1175, 1068, 818; m.p.: 197°C (lit.⁴⁰ 197); UV-vis (CH₃CN): λ_{max}(ε) = 311 (22700 L.cm⁻¹.mol⁻¹); Φ_F=0.09 in CH₃CN; τ=10.38 ns; E° (C, CH₂Cl₂) vs. ferrocene: 0.85 V.

***N,N,N*-tri-(4-methoxyphenyl)amine 4:** In a Schlenk flask under argon 4-bromoanisole (6.3 mL, 50 mmol, 3.1 eq) was added to a solution of tris(dibenzylideneacetone)dipalladium(0) Pd₂(dba)₃ (857 mg, 0.936 mmol, 0.06 eq) and 1,1'-bis(diphenylphosphino)ferrocene DPPF (801 mg, 1.47 mmol, 0.09 eq) in toluene (55 mL). The mixture was stirred at room temperature for 10 minutes and then were added sodium *tert*-butoxyde (4.06 g, 42.2 mmol, 2.6 eq) and *p*-anisidine (2.00 g, 16.2 mmol, 1.0 eq). The mixture was heated at 90°C for 24 hours. After the mixture was cooled down, dichloromethane (200 mL) and water (200 mL) were added. Organic compounds were extracted with dichloromethane (3*150 mL). The combined organic phases were dried over anhydrous sodium sulfate, filtrated and concentrated under reduced pressure. The crude product was purified by silica gel flash chromatography [DCM/PE (5/5) to DCM] to give **4** (1.62 g, 30 %) as white solid. ¹H NMR (400 MHz, CDCl₃) δ (ppm): 6.94 (d, J=8.7 Hz, 6H), 6.82 (d, J=8.7 Hz, 6H), 3.78 (s, 9H); ¹³C NMR (100 MHz, CDCl₃) δ (ppm): 154.3, 138.0, 119.6, 114.8, 55.8; IR (σ in cm⁻¹): 2954, 1521, 1241, 1227, 1032, 830, 818; m.p.: 108°C (lit.⁷³ 102); UV-vis (CH₃CN): λ_{max}(ε) = 283 (25500 L.cm⁻¹.mol⁻¹);

Φ_F=0.06 in CH₃CN; τ=3.64 ns; E° (C, CH₂Cl₂) vs. ferrocene: 0.17 V.

***N,N*-ditolyl-4-anisidine 5:** To a solution of tris(dibenzylideneacetone)dipalladium(0) Pd₂(dba)₃ (120 mg, 0.131 mmol) and 1,1'-bis(diphenylphosphino)ferrocene DPPF (140 mg, 0.258 mmol) in dried toluene (35 mL) under argon atmosphere was added 4-bromotoluene (4 mL, 32.5 mmol) at room temperature. The resulting mixture was stirred for 10 minutes. Then sodium *tert*-butoxyde (2.070 g, 21.54 mmol) and 4-anisidine (0.99 g, 8.04 mmol) were added. The resulting mixture was stirred at 110°C for 19 hours then cooled to room temperature and concentrated under reduced pressure. The crude product was purified by a silica gel column chromatography (petroleum ether/CH₂Cl₂ (8/2) until petroleum ether/CH₂Cl₂ (5/5)) to give 2.048 g of a grey solid (93 %). ¹H NMR (400 MHz, CDCl₃): δ (ppm)=7.08-7.05 (m, 6H), 6.97 (d, J=8.2 Hz, 4H), 6.84 (d, J=8.7 Hz, 2H), 3.82 (s, 3H), 2.33 (s, 6H); ¹³C NMR (100 MHz, CDCl₃): δ (ppm)=155.7, 146.0, 141.4, 131.3, 129.8, 126.5, 123.2, 114.7, 55.5, 20.8; IR (cm⁻¹): 3024-2830, 1606, 1499, 1273, 812; m.p.: 70°C (lit.⁷⁴ 70-73); UV-vis (CH₃CN): λ_{max}(ε) = 301 (25000 L.cm⁻¹.mol⁻¹); Φ_F=0.03 in CH₃CN; τ=5.22, 1.78 ns; E° (C, CH₂Cl₂) vs. ferrocene: 0.22 V

***N,N,N*-tri-(4'-methoxy-1,1'-biphenyl)amine 6:** In a Schlenk flask under argon tetrakis(triphenylphosphine) Pd(PPh₃)₄ (98 mg, 0.085 mmol, 0.1 eq) was added to a solution of *N,N,N*-tri-(4-bromophenyl)amine (413 mg, 0.857 mmol, 1.0 eq) in toluene (20 mL). The mixture was stirred at room temperature for 15 minutes and then were added solutions of 4-methoxyphenylboronic acid (673 mg, 4.43 mmol, 5.2 eq) in methanol (6.5 mL), of sodium carbonate (561 mg, 5.29 mmol, 6.2 eq) in distilled water (2.5 mL). The mixture was heated at 80°C for 84 hours. After the mixture was cooled down, dichloromethane (50 mL) and saturated ammonium chloride solution (50 mL) were added. Organic compounds were extracted with dichloromethane (3*50 mL). The combined organic phases were dried over anhydrous sodium sulfate, filtrated and concentrated under reduced pressure. The crude product was purified by silica gel flash chromatography [DCM/PE (5/5)] to give **6** (305 mg, 63 %) as a white solid. ¹H NMR (400 MHz, DMSO) δ (ppm): 7.59 (d, J=8.7 Hz, 6H), 7.58 (d, J=8.7 Hz, 6H), 7.12 (d, J=8.7 Hz, 6H), 7.00 (d, J=9.2 Hz, 6H), 3.78 (s, 9H); ¹³C NMR (100 MHz, DMSO) δ (ppm): 159.0, 146.5, 135.3, 133.4, 127.8, 127.5, 124.5, 114.3, 55.5; IR (σ in cm⁻¹): 2991, 2965, 1391, 1252, 1061; m.p.: 200°C (lit.⁷⁵ 237-240); UV-vis (CH₃CN): λ_{max}(ε) = 357 (54300 L.cm⁻¹.mol⁻¹); Φ_F=0.37 in CH₃CN; τ=9.95 ns; E° (C, CH₂Cl₂) vs. ferrocene: 0.25 V.

bis(4-bromophenyl)phenylamine 7: To a solution of bis(4-bromophenyl)amine (7.57 g, 23.1 mmol, 1.0 eq) in toluene (50 mL) were added cyclohexane-1,4-dione (2.80 g, 25.0 mmol, 1.1 eq) and *p*-toluene sulfonic acid (0.53 g, 0.31 mmol, 0.01 eq). The mixture was stirred at reflux with a Dean-Stark apparatus for 9 hours then concentrated under reduced pressure. The crude product was purified by a silica gel flash chromatography [DCM/PE (1/9)] to give **7** (5.77 g, 62%) as colorless oil. ¹H

NMR (400 MHz, CDCl_3) δ (ppm): 7.33 (d, $J=8.7$ Hz, 4H), 7.26 (dd, $J=7.8$ and 7.8 Hz, 2H), 7.06 (m, 3H), 6.23 (d, $J=8.7$ Hz, 4H); ^{13}C NMR (100 MHz, CDCl_3) δ (ppm): 147.0, 147.7, 132.5, 129.7, 125.5, 124.7, 123.9, 115.6; IR (σ in cm^{-1}): 1580, 1483, 1311, 1286, 1272, 1069, 1009, 841, 823, 813.

4-(*N,N*-diphenylamino)benzaldehyde 8: To a solution of phosphorus oxychloride (1.85 mL, 20 mmol, 1 eq) in dimethylformamide (5.6 mL, 73 mmol, 3.7 eq) at 0°C under argon was added triphenylamine (5.00 g, 20 mmol, 1.0 eq). The mixture was stirred at 70°C for 24h. The mixture was then poured into the ice and neutralised with saturated sodium carbonate solution (20 mL). The aqueous layer was extracted with CH_2Cl_2 (3*20 mL). The organic layer was dried over anhydrous sodium sulfate, filtered and concentrated under reduced pressure. The crude product was purified by a silica gel flash chromatography [DCM] to give **8** (4.22 g, 77 %) as yellow solid. ^1H NMR (400 MHz, CDCl_3) δ (ppm): 9.80 (s, 1H), 7.67 (d, $J=8.7$ Hz, 2H), 7.34 (dd, $J=7.8$ and 7.8 Hz, 4H), 7.16 (m, 6H), 7.01 (d, $J=8.7$ Hz, 2H); ^{13}C NMR (100 MHz, CDCl_3) δ (ppm): 190.6, 153.5, 146.3, 131.4, 129.9, 129.2, 126.4, 125.2, 119.5; IR (σ in cm^{-1}): 1687, 1583, 1504, 1488, 1330, 1304, 1289, 1220, 1155, 824; m.p.: 132°C (lit.⁷⁶ 132).

4-[*N,N*-di-(4'-bromophenyl)amino]benzaldehyde oxime 9: To a solution of 4-[*N,N*-di-(4'-bromophenyl)amino]benzaldehyde **1** (0.80 g, 1.8 mmol, 1 eq) in dichloromethane (8 mL) was added a solution of hydroxylamine hydrochloride (0.52 g, 7.4 mmol, 4 eq) and sodium acetate (0.76 g, 9.3 mmol, 5 eq) in ethanol (24 mL). The mixture was stirred at room temperature for 3h and concentrated under reduced pressure. The crude product was purified by a silica gel flash chromatography [DCM/PE (1/9) to DCM/EtOH (9.7/0.3)] to give **9** (0.80 g, 97 %) as white solid. ^1H NMR (400 MHz, CDCl_3) δ (ppm): 8.44 (s, 1H), 8.08 (s, 1H), 7.44 (d, $J=8.7$ Hz, 2H), 7.37 (d, $J=8.7$ Hz, 4H), 7.01 (d, $J=8.2$ Hz, 2H), 6.96 (d, $J=8.7$ Hz, 4H); ^{13}C NMR (100 MHz, CDCl_3) δ (ppm): 149.7, 148.6, 145.9, 132.7, 128.3, 126.5, 126.3, 123.1, 116.6; IR (σ in cm^{-1}): 3289, 1605, 1581, 1513, 1486, 1313, 1289, 1069, 926, 907, 871, 823; m.p.: 104°C ; MS: calcd. for $\text{C}_{19}\text{H}_{14}^{79}\text{Br}_2\text{N}_2\text{O}$ [$\text{M}+\text{H}$] $^+$ 444.9546, found 444.9555.

Acknowledgements

We thank the CNRS and the Ministry of French Research for funding the project. We also thank Dr C. Allain for fruitful discussions.

Notes and references

^a PPSM, CNRS UMR8531, ENS Cachan, UniverSud
61 Avenue du Président Wilson, 94235 Cachan, France
Fax: (+) 33-1-47402454

Electronic Supplementary Information (ESI) available: [electrochemical data, fluorescence switching experiments, theoretical calculations, NMR characterizations]. See DOI: 10.1039/b000000x/

1. P. Audebert and F. Miomandre, *Chem. Sci.*, 2013, **4**, 575.

- C. Amatore, S. Arbault, Y. Chen, C. Crozatier, F. Lemaître and Y. Verchier, *Angew. Chem., Int. Ed.*, 2006, **45**, 4000.
- B. X. Shi, Y. Wang, T. L. Lam, W. H. Huang, K. Zhang, Y. C. Leung and H. L. Chan, *Biomicrofluidics*, 2010, **4**, 43009.
- A. Meunier, O. Jouannot, R. Fulcrand, I. Fanget, M. Bretou, E. Karatekin, S. Arbault, M. Guille, F. Darchen, F. Lemaître and C. Amatore, *Angew. Chem. Int. Ed.*, 2011, **50**, 5081-5084.
- Y. Kim, E. Kim, G. Clavier and P. Audebert, *Chem. Commun.*, 2006, 3612-3614.
- Y. Kim, J. Do, E. Kim, G. Clavier, L. Galmiche and P. Audebert, *J. Electroanal. Chem.*, 2009, **632**, 201.
- S. Seo, Y. Kim, Q. Zhou, G. Clavier, P. Audebert and E. Kim, *Adv. Funct. Mater.*, 2012, **22**, 3556-3561.
- S. Seo, Y. Kim, J. You, B. D. Sarwade, P. P. Wadgaonkar, S. K. Menon, A. S. More and E. Kim, *Macromol. Rapid Commun.*, 2011, **32**, 637-643.
- D. Canevet, M. Salle, G. Zhang, D. Zhang and D. Zhu, *Chem. Commun.*, 2009, 2245-2269.
- C. Quinton, V. Alain-Rizzo, C. Dumas-Verdes, G. Clavier, F. Miomandre and P. Audebert, *Eur. J. Org. Chem.*, 2012, 1394-1403.
- C. Quinton, V. Alain-Rizzo, C. Dumas-Verdes, F. Miomandre and P. Audebert, *Electrochim. Acta*, 2013, **110**, 693-701.
- Y.-X. Yuan, Y. Chen, Y.-C. Wang, C.-Y. Su, S.-M. Liang, H. Chao and L.-N. Ji, *Inorg. Chem. Commun.*, 2008, **11**, 1048-1050.
- A. C. Benniston, G. Copley, K. J. Elliot, R. W. Harrington and W. Clegg, *Eur. J. Org. Chem.*, 2008, 2705.
- R. A. Illos, D. Shamir, L. J. W. Shimon, I. Zilbermann and S. Bittner, *Tetrahedron Lett.*, 2006, **47**, 5543-5546.
- R. Zhang, Z. Wang, Y. Wu, H. Fu and J. Yao, *Org. Lett.*, 2008, **10**, 3065-3068.
- R. Martinez, I. Ratera, A. Tarraga, P. Molina and J. Veciana, *Chem. Commun.*, 2006, 3809-3811.
- K. Nakamura, K. Kanazawa and N. Kobayashi, *Chem. Commun.*, 2011, **47**, 10064-10066.
- R. A. Illos, E. Harlev and S. Bittner, *Tetrahedron Lett.*, 2005, **46**, 8427-8430.
- M. Dias, P. Hudhomme, E. Levillain, L. Perrin, Y. Sahin, F. X. Sauvage and C. Wartelle, *Electrochem. Commun.*, 2004, **6**, 325.
- F. Miomandre, E. Lépicier, S. Munteanu, O. Galangau, J. F. Audibert, R. Méallet-Renault, P. Audebert and R. B. Pansu, *ACS Appl. Mater. Interfaces*, 2011, **3**, 690-696.
- F. Miomandre, C. Allain, G. Clavier, J.-F. Audibert, R. B. Pansu, P. Audebert and F. Hartl, *Electrochem. Commun.*, 2011, **13**, 574-577.
- C. Dumas-Verdes, F. Miomandre, E. Lépicier, O. Galangau, T. T. Vu, G. Clavier, R. Méallet-Renault and P. Audebert, *Eur. J. Org. Chem.*, 2010, **2010**, 2525-2535.
- H. Li, J. O. Jeppesen, E. Levillain and J. Becher, *Chem. Commun.*, 2003, 846-847.
- J. Yoo, T. Kwon, B. D. Sarwade, Y. Kim and E. Kim, *Appl. Phys. Lett.*, 2007, **91**, 241107.
- S. Beaupré, J. Dumas and M. Leclerc, *Chem. Mater.*, 2006, **18**, 4011-4018.

26. S.-H. Hisiao, G.-S. Liou, Y.-C. Kung and H.-J. Yen, *Macromolecules*, 2008, **41**, 2800-2808.
27. G. Nursalim and Y. Chen, *Polymer*, 2010, **51**, 3187-3195.
28. A. Ito, D. Sakamaki, Y. Ichikawa and K. Tanaka, *Chem. Mater.*, 2011, **23**, 841-850.
29. C.-Y. Huang, C.-Y. Hsu, L.-Y. Yang, C.-J. Lee, T.-F. Yang, C.-C. Hsu, C.-H. Ke and Y. O. Su, *Eur. J. Inorg. Chem.*, 2012, 1038-1047.
30. X. Cheng, J. Zhao, C. Cui, Y. Fu and X. Zhang, *J. Electroanal. Chem.*, 2012, **677-680**, 24-30.
31. C. Xu, J. Zhao, C. Cui, M. Wang, Y. Kong and X. Zhang, *J. Electroanal. Chem.*, 2012, **682**, 29-36.
32. S. J. Yeh, C. Y. Tsai, H. C.-Y., G.-S. Liou and S.-H. Cheng, *Electrochem. Commun.*, 2003, **5**, 373-377.
33. L.-T. Huang, H.-J. Yen, J.-H. Wu and G.-S. Liou, *Org. Electron.*, 2012, **13**, 840-849.
34. G.-S. Liou, S.-H. Hsiao, N.-K. Huang and Y.-L. Yang, *Macromolecules*, 2006, **39**, 5337-5346.
35. A. J. Wain, I. Streeter, M. Thompson, N. Fietkau, L. Drouin, A. J. Fairbanks and R. G. Compton, *J. Phys. Chem. B*, 2006, **110**, 2681-2691.
36. S. Barlow, C. Risko, S. A. Odom, S. Zheng, V. Coropceanu, L. Beverina, J.-L. Brédas and S. R. Marder, *J. Am. Chem. Soc.*, 2012, **134**, 10146-10155.
37. B. Li, Q. Li, B. Liu, Y. Yue and M. Yu, *Dyes Pigm.*, 2011, **88**, 301-306.
38. T. Duan, K. Fan, Y. Fu, C. Zhong, X. Chen, T. Peng and J. Qin, *Dyes Pigm.*, 2012, **94**, 28-33.
39. Y.-D. Lin, C.-T. Chien, S.-Y. Lin, H.-H. Chang, C.-Y. Liu and T. J. Chow, *J. Photochem. Photobiol., A*, 2011, **222**, 192-202.
40. E. n. Ishow, A. Brosseau, G. Clavier, K. Nakatani, P. Tauc, C. I. Fiorini-Debuisschert, S. Neveu, O. Sandre and A. Léaustic, *Chem. Mater.*, 2008, **20**, 6597-6599.
41. C.-P. Kuo, Y.-S. Lin and M.-k. Leung, *J. Polym. Sci., Part A: Polym. Chem.*, 2012, **50**, 5068-5078.
42. J. Louie and J. F. Hartwig, *Tetrahedron Lett.*, 1995, **36**, 3609-3612.
43. A. S. Guram, R. A. Rennels and S. L. Buchwald, *Angew. Chem. Int. Ed.*, 1995, **34**, 1348-1350.
44. A. C. Hernandez-Perez and S. K. Collins, *Angewandte Chemie International Edition*, 2013, **52**, 12696-12700.
45. J. F. Hartwig, M. Kawatsura, S. I. Hauck, K. H. Shaughnessy and L. M. Alcazar-Roman, *J. Org. Chem.*, 1999, **64**, 5575-5580.
46. K. Haga, K. Iwaya and R. Kaneko, *Bull. Chem. Soc. Jpn.*, 1986, **59**, 803-807.
47. K. Haga, M. Oohashi and R. Kaneko, *Bull. Chem. Soc. Jpn.*, 1984, **57**, 1586-1590.
48. Q. Fang and T. Yamamoto, *Macromolecules*, 2004, **37**, 5894-5899.
49. J. H. Seok, S. H. Park, M. E. El-Khouly, Y. Araki, O. Ito and K.-Y. Kay, *J. Organomet. Chem.*, 2009, **694**, 1818-1825.
50. K. Takahashi, T. Furusawa, T. Sawamura, S. Kuribayashi, S. Inagi and T. Fuchigami, *Electrochim. Acta*, 2012, **77**, 47-53.
51. G. Lai, X. R. Bu, J. Santos and E. A. Mintz, *Synlett*, 1997, **1997**, 1275-1276.
52. L. Ji, Q. Fang, M.-S. Yuan, Z.-Q. Liu, Y.-X. Shen and H.-F. Chen, *Org. Lett.*, 2010, **12**, 5192-5195.
53. N. B. McKeown, S. Badriya, M. Helliwell and M. Shkunov, *J. Mater. Chem.*, 2007, **17**, 2088.
54. Y.-J. Chen and C. Chen, *Tetrahedron: Asymmetry*, 2008, **19**, 2201-2209.
55. N. D. Kokare and D. B. Shinde, *Monatshefte für Chemie - Chemical Monthly*, 2008, **140**, 185-188.
56. S.-T. Liu, H.-P. Chen, Y.-T. Li and B.-S. Liao, *Synthesis*, 2011, **2011**, 2639-2643.
57. S. Enthaler, M. Weidauer and F. Schröder, *Tetrahedron Lett.*, 2012, **53**, 882-885.
58. R. M. Denton, J. An, P. Lindovska and W. Lewis, *Tetrahedron*, 2012, **68**, 2899-2905.
59. B. Thomas, S. Prathapan and S. Sugunan, *Chem. Eng. J.*, 2007, **133**, 59-68.
60. N. Miyaura and A. Suzuki, *Chem. Rev.*, 1995, **95**, 2457.
61. S. C. Creason, J. Wheeler and R. F. Nelson, *J. Org. Chem.*, 1972, **37**, 4440-4446.
62. J.-H. Pan, H.-L. Chiu, L. Chen and B.-C. Wang, *Comput. Mater. Sci.*, 2006, **38**, 105-112.
63. L. Ebersson and B. Larsson, *Acta Chem. Scand.*, 1987, **41**, 367-378.
64. J. N. Demas, *Opt. Radiat. Meas.*, 1982, **3**, 195.
65. E. Ishow, G. Clavier, F. Miomandre, M. Rebarz, G. Buntinx and O. Poizat, *Physical chemistry chemical physics : PCCP*, 2013, **15**, 13922-13939.
66. C.-C. Chang, H. Yueh and C.-T. Chen, *Org. Lett.*, 2011, **13**, 2702-2705.
67. K. Sreenath, C. V. Suneesh, K. R. Gopidas and R. A. Flowers, *J. Phys. Chem. A*, 2009, **113**, 6477-6483.
68. K. Sreenath, C. V. Suneesh, V. K. Ratheesh Kumar and K. R. Gopidas, *J. Org. Chem.*, 2008, **73**, 3245-3251.
69. C. Quinton, V. Alain-Rizzo, C. Dumas-Verdes, F. Miomandre, G. Clavier and P. Audebert, *Chem. Eur. J.*
70. C. Adamo and D. Jacquemin, *Chem. Soc. Rev.*, 2013, **42**, 845-856.
71. M. Krejčík, M. Daněk and F. Hartl, *J. Electroanal. Chem. Interfacial Electrochem.*, 1991, **317**, 179-187.
72. M. W. Thesen, B. Höfer, M. Debeaux, S. Janietz, A. Wedel, A. Köhler, H.-H. Johannes and H. Krueger, *J. Polym. Sci., Part A: Polym. Chem.*, 2010, **48**, 3417-3430.
73. T. Kurata, K. Koshika, F. Kato, J. Kido and H. Nishide, *Polyhedron*, 2007, **26**, 1776-1780.
74. Y.-H. Liu, C. Chen and L.-M. Yang, *Tetrahedron Lett.*, 2006, **47**, 9275-9278.
75. H. Yu, C. Shen, M. Tian, J. Qu and Z. Wang, *Macromolecules*, 2012, **45**, 5140-5150.
76. M. E. El-Khouly, D. K. Ju, K. Y. Kay, F. D'Souza and S. Fukuzumi, *Chem. Eur. J.*, 2010, **16**, 6193-6202.

